Sensitivity Analysis Based Preform Die Shape Design Using the Finite Element Method

G.Q. Zhao, R. Huff, A. Hutter, and R.V. Grandhi

This paper uses a finite element-based sensitivity analysis method to design the preform die shape for metal forming processes. The sensitivity analysis was developed using the rigid visco-plastic finite element method. The preform die shapes are represented by cubic B-spline curves. The control points or coefficients of the B-spline are used as the design variables. The optimization problem is to minimize the difference between the realized and the desired final forging shapes. The sensitivity analysis includes the sensitivities of the objective function, nodal coordinates, and nodal velocities with respect to the design variables. The remeshing procedure and the interpolation/transfer of the history/dependent parameters are considered. An adjustment of the volume loss resulting from the finite element analysis is used to make the workpiece volume consistent in each optimization iteration and improve the optimization convergence. In addition, a technique for dealing with fold-over defects during the forming simulation is employed in order to continue the optimization procedures of the preform die shape design. The method developed in this paper is used to design the preform die shape for both plane strain and axisymmetric deformations with shaped cavities. The analysis shows that satisfactory final forging shapes are obtained using the optimized preform die shapes.

Keywords

finite element method, forging, optimization, preform design, sensitivity analysis

1. Introduction

METAL FORMING TECHNOLOGY is very important in today's modern industry. Die design is an important step of metal forming process design for maintaining the overall quality control of products and minimizing material waste. The reduction of die design/manufacture cost where preform die shape design is critical and challenging work is also an important aspect of die design. The innovation and replacement of products requires fast and exact die design. Engineering experience and intuition based die design has not satisfied the requirements of rapidly developing industry. Computer-aided simulation using the finite element method has played an important role in metal forming process design over the last decade. It has also provided us with an opportunity for developing new methods for process sequence and preform die shape design.

Kobayashi et al. (Ref 1) introduced a finite element method that simulated metal forming processes in reverse to design the preform die shapes. The process known as backward tracing was applied to several practical forging problems (Ref 2-4). Zhao et al. (Ref 5, 6) established a node detachment criterion for backward simulation and the related preform design according to forging shape complexity control and applied this method in preform design of axisymmetric deformation problems. Zhao et al. (Ref 7) also gave an inverse die contact tracking method for designing the preform shapes.

All of these methods use both forward and backward simulations and rely on selecting the appropriate detachment criteria of boundary nodes during the backward simulation. Unfortunately, there are no all-purpose boundary node detachment criteria currently available. In each case, the design objectives were the preform or intermediate forging shapes rather then directly designing the preform die shapes, so the preform die shape then had to be designed to produce the preform shape of the workpiece.

Badrinarayanan and Zabaras (Ref 8) developed a sensitivity analysis method for large deformation of hyperelastic visco-plastic solids that can be applied to preform design problems in metal forming. Like the backward tracing technique, this method designs the preform or intermediate shape of the workpiece instead of preform die shapes. Their method was applied to an axisymmetric disk upsetting problem where the preform is designed such that a final forging with a minimum barreling effect is achieved. The desired results were achieved; however, the axisymmetric preform shape had a concave lateral shape that is very difficult to forge.

Fourment et al. (Ref 9) described a method to design the preform tools and the preform shapes. The distance between the achieved and required part is used as the objective function to be minimized. The shapes are discretized using spline functions. The design variables of the optimization problem are the displacements of the selected characteristic points of the spline in the normal direction. The gradients are calculated analytically where the friction on the tool-workpiece interface is considered as the exponential function of the sliding velocity. The shape optimization for both one- and two-step forging operations was performed using this method.

Zhao et al. (Ref 10, 11) focused on optimal design of the preform die shapes instead of the preform shapes and developed an optimization method for preform die shape design in metal forming using forward simulation only. The preform die shapes are represented using a piecewise cubic B-spline function. The objective is to reduce the area of the zone where the achieved final forging shape and desired final forging shape do not coincide. B-spline coefficients are considered as the design variables for the sensitivity analysis and optimization problem.

G.Q. Zhao, Department of Materials Engineering, Shandong University of Technology, Jinan, Shandong 250061, China; and **R. Huff, A. Hutter,** and **R.V. Grandhi,** Department of Mechanical and Material Engineering, Wright State University, Dayton, OH 45435, USA.

The required sensitivity analysis for rigid-plastic or visco-rigid plastic deformation problems is developed in detail, including the velocity boundary conditions for the contact problem. The method was demonstrated using an upsetting process and an H-shaped forging with a shallow cavity, demonstrating plane strain and axisymmetric deformation problems.

This paper is the extension of the previous work (Ref 10, 11). The sensitivity analysis and related preform die shape design methods are applied in more complex forging problems, which include remeshing and the occurrence of a fold-over defect.

2. Optimization Problem

In this paper, only the major equations related to sensitivity analysis and optimization of preform die design are presented. Further detail of the methodology and equations is included in Ref 10 and 11.

Different preform die shapes generate different final forging shapes in a multistage forging process. The final forging shape achieved using any preform die shape is referred to as the achieved final forging shape. The desired final forging has complete die fill with the minimum amount of flash possible. For two-dimensional metal forming processes, it is the design goal to make the achieved final forging shape as close as possible to the desired final forging shape by designing the proper preform dies. The objective function or difference of two shapes can be expressed as the area of the zone where the two shapes do not coincide.

For the discretized boundaries of the workpiece, suppose there are N boundary nodes around the achieved final shape with coordinates (x_i, y_i) $(i = 1, 2, \ldots, N)$. Similarly, the boundary of the desired shape can be discretized by extending a line in the normal direction from each node on the achieved shape boundary to intersect the desired shape boundary. This provides a second set of node coordinates for the desired shape (x_0, y_0) $(i = 1, 2, \ldots, N)$. By connecting two consecutive nodes from each boundary, a number of quadrilateral elements are generated. These elements represent the zone(s) where the two shapes are different. In this way, the objective function can be expressed as:

$$\psi = \left(\sum_{j=1}^{N} A_j \right)^2 \qquad \text{(Eq 1)}$$

where A_j is the area of the jth element in the zone. When ψ approaches zero, the achieved shape will be consistent with the desired shape. Therefore, the optimization problem is to define the preform die shapes that will minimize the objective function ψ.

The shapes of the preform dies for a two-dimensional problem can be represented using cubic B-spline functions. The B-spline shapes are controlled by varying the coefficients or the coordinates of the control points. For each control point, there are two degrees of freedom (p_{x_i}, p_{y_i}) $i = 1, 2, \ldots, K$ for a total of $2K$ design variables. For this unconstrained problem, the Broyden Fletcher Goldfarb Shanno (BFGS) algorithm (Ref 12) is used to minimize the objective function ψ with respect to the design variables p_l.

3. Sensitivity Analysis

According to the objective function given in Eq 1, the gradient of the objective function ψ with respect to the design variable p_l is obtained as follows:

$$\frac{\partial \psi}{\partial p_l} = \sum_{i=1}^{N} \frac{\partial \psi}{\partial x_i} \frac{\partial x_i}{\partial p_l} + \sum_{i=1}^{N} \frac{\partial \psi}{\partial y_i} \frac{\partial y_i}{\partial p_l} \qquad (l = 1, 2, \ldots, 2K) \text{ (Eq 2)}$$

where $\partial\psi/\partial x_i$ and $\partial\psi/\partial y_i$ can be obtained by differentiating the objective function ψ with respect to the coordinates x_i and y_i according to the objective function (Eq 1). The sensitivities of the nodal coordinates with respect to the design variables, $\partial x_i/\partial p_l$ and $\partial y_i/\partial p_l$, need to be derived from the finite element stiffness equation of the forging problem.

After convergence of the finite element analysis, the velocity field at the incremental simulation step is used to update the nodal coordinates using:

$$\mathbf{X}^{(t+\Delta t)} = \mathbf{X}^{(t)} + \mathbf{V}^{(t)} \Delta t \qquad \text{(Eq 3)}$$

where $\mathbf{X}^{(t+\Delta t)}$ is the nodal coordinate vector at time $t + \Delta t$. $\mathbf{X}^{(t)}$ is the nodal coordinate vector at time t, and $\mathbf{V}^{(t)}$ is the nodal velocity vector at time t. Differentiation of Eq 3 with respect to the design variables p_l results in:

$$\frac{\partial \mathbf{X}^{(t+\Delta t)}}{\partial p_l} = \frac{\partial \mathbf{X}^{(t)}}{\partial p_l} + \frac{\partial \mathbf{V}^{(t)}}{\partial p_l} \Delta t \qquad \text{(Eq 4)}$$

It can be seen from Eq 1 and 4 that the gradients of the objective function with respect to the design variables can be computed once the sensitivities of the nodal velocities with respect to the design variables are available.

3.1 *Velocity Sensitivity* $\partial \mathbf{V}^{(t)}/\partial p_l$

The elemental stiffness equation of the forging problem using finite element modeling (FEM) can be expressed as:

$$\mathbf{K}(\mathbf{V},\mathbf{X})\mathbf{V} + \mathbf{F}(\mathbf{V},\mathbf{X}) = 0 \qquad \text{(Eq 5)}$$

where

$$K_{ij}(\mathbf{V},\mathbf{X}) = \int_V \frac{\bar{\sigma}}{\dot{\bar{\varepsilon}}} P_{ij}\, dV + Q \int_V C_i C_j\, dV \qquad \text{(Eq 6a)}$$

$$F_i(\mathbf{V},\mathbf{X}) = \int_{S_c} mk\frac{2}{\pi} q_i \tan^{-1}\left(\frac{q_j u_{sj}}{u_0}\right) dS \qquad \text{(Eq 6b)}$$

where $\mathbf{K}$ is the material and process dependent nonlinear stiffness matrix, and $\mathbf{F}$ is the applied nodal point force vector. $\mathbf{X}$ is the nodal coordinate vector of the element. Q is a large positive constant that penalizes the dilatational strain in the rigid-plastic formulation. q_j are the element shape functions expressed in the natural coordinate system (ξ, η). $\bar{\sigma}$ is the effective stress. $\dot{\bar{\varepsilon}}$ is the effective strain rate. k is the shear yield stress, and m is the constant friction factor. u_{sj} is the relative sliding velocity at node j on the die-workpiece contact interface. u_0 is a small positive number compared to u_s. P_{ij} is an element of effective strain rate matrix, $\mathbf{P}$, and C_i is an element of volumetric strain rate vector, $\mathbf{C}$.

The nodal velocity sensitivities $V_{,p_l}$ at time t are obtained by differentiating the equilibrium equation (Eq 5) respect to the design variable p_l at the elemental level.

$$\left(\frac{\partial \mathbf{K}}{\partial \mathbf{V}}\mathbf{V} + \mathbf{K} + \frac{\partial \mathbf{F}}{\partial \mathbf{V}}\right)\frac{\partial \mathbf{V}}{\partial p_l} = -\left(\frac{\partial \mathbf{K}}{\partial \mathbf{X}}\frac{\partial \mathbf{X}}{\partial p_l}\mathbf{V} + \frac{\partial \mathbf{F}}{\partial \mathbf{X}}\frac{\partial \mathbf{X}}{\partial p_l}\right) \qquad \text{(Eq 7a)}$$

Equation 7a can be simply rewritten as:

$$\mathbf{R}\mathbf{V}_{,p_l} = \mathbf{F}_{,p_l} \qquad \text{(Eq 7b)}$$

where $\mathbf{R}$ is the elemental stiffness matrix sensitivity (8×8), $\mathbf{F}_{,p_l}$ is the elemental force vector sensitivity, and $\mathbf{V}_{,p_l}$ is the sensitivity vector of the nodal velocities with respect to the lth design variable. The components of the matrix $\mathbf{R}$ and vector $\mathbf{F}_{,p_l}$ are expressed as:

$$R_{ij} = \sum_{n=1}^{8}\sum_{m=1}^{8}\int_V \left(\frac{1}{\dot{\bar{\varepsilon}}}\frac{\partial \bar{\sigma}}{\partial \dot{\bar{\varepsilon}}} - \frac{\bar{\sigma}}{\dot{\bar{\varepsilon}}^2}\right)\frac{1}{\dot{\bar{\varepsilon}}} P_{in} v_n v_m P_{mj}\, dV + K_{ij} + \frac{\partial F_i}{\partial v_j}$$
$$(i,j = 1, 2, \ldots, 8) \qquad \text{(Eq 8a)}$$

$$F_{i,p_l} = -\left(\sum_{n=1}^{8}\frac{\partial F_i}{\partial x_n}\frac{\partial x_n}{\partial p_l} + \sum_{j=1}^{8}\sum_{n=1}^{8}\frac{\partial K_{ij}}{\partial x_n}\frac{\partial x_n}{\partial p_l} v_j\right)$$
$$(i = 1, 2, \ldots, 8) \qquad \text{(Eq 8b)}$$

According to Eq 6(a) and (b), the derivatives $\partial K_{ij}/\partial x_n$, $\partial F_i/\partial x_n$, and $\partial F_i/\partial v_j$ in Eq 8(a) and (b) at the elemental level are developed as follows:

$$\frac{\partial F_i}{\partial v_j} = \int_S mk\frac{2}{\pi} q_i q_j \frac{u_0}{u_0^2 + (q_k u_{sk})^2}\, dS \qquad \text{(Eq 9)}$$

$$\frac{\partial F_i}{\partial x_n} = \sum_{\alpha=1}^{8}\sum_{k=1}^{8}\int_S \frac{m}{\sqrt{3}\pi}\frac{\partial \bar{\sigma}}{\partial \dot{\bar{\varepsilon}}} q_i \frac{1}{\dot{\bar{\varepsilon}}} v_\alpha \frac{\partial P_{\alpha k}}{\partial x_n} v_k \tan^{-1}\left(\frac{q_j u_{sj}}{u_0}\right) dS$$
$$+ \int_{S_c} mk\frac{2}{\pi} q_i \tan^{-1}\left(\frac{q_j u_{sj}}{u_0}\right)\frac{\partial (dS)}{\partial x_n} \qquad \text{(Eq 10)}$$

$$\frac{\partial K_{ij}}{\partial x_n} = \int_V \left(\frac{1}{\dot{\bar{\varepsilon}}}\frac{\partial \bar{\sigma}}{\partial \dot{\bar{\varepsilon}}} - \frac{\bar{\sigma}}{\dot{\bar{\varepsilon}}^2}\right)\frac{1}{2\dot{\bar{\varepsilon}}}\frac{\partial (\mathbf{V}^T\mathbf{P}\mathbf{V})}{\partial x_n} P_{ij} dV$$
$$+ \int_V \frac{\bar{\sigma}}{\dot{\bar{\varepsilon}}}\frac{\partial P_{ij}}{\partial x_n} dV + Q\int_V \frac{\partial C_i}{\partial x_n} C_j dV + Q\int_V C_i \frac{\partial C_j}{\partial x_n} dV$$
$$+ \int_V \frac{\bar{\sigma}}{\dot{\bar{\varepsilon}}} P_{ij}\frac{\partial (dV)}{\partial x_n} + Q\int_V C_i C_j \frac{\partial (dV)}{\partial x_n} \qquad \text{(Eq 11)}$$

where $\partial C_i/\partial x_n$, $\partial C_j/\partial x_n$, $\partial P_{ij}/\partial x_n$, and $\partial(\mathbf{V}^T\mathbf{P}\mathbf{V})/\partial x_n$ can be obtained according to expressions of the volumetric strain rate vector $\mathbf{C}$, the effective strain rate matrix $\mathbf{P}$, and the strain rate matrix $\mathbf{B}$.

In addition, the differential volume dV and area dS are also dependent on the nodal coordinate vector $\mathbf{X}$. By using the natural coordinates $(-1 \le \xi \le 1, -1 \le \eta \le 1)$ in the two-dimensional space, $\partial(dS)/\partial x_n$ and $\partial(dV)/\partial x_n$ can be represented as follows. For a plane strain problem:

$$\frac{\partial (dS)}{\partial x_n} = \frac{\partial |\mathbf{J}_s|}{\partial x_n} d\xi$$
$$\frac{\partial (dV)}{\partial x_n} = \frac{\partial |\mathbf{J}|}{\partial x_n} d\xi d\eta$$

where $|\mathbf{J}_s|$ is the determinant of the Jacobian of the coordinate transformation matrix on the die-workpiece interface. $|\mathbf{J}|$ is the determinant of the Jacobian matrix.

For an axisymmetric problem:

$$\frac{\partial (dS)}{\partial x_n} = \frac{\partial (r|\mathbf{J}_s|)}{\partial x_n} d\xi = \left(|\mathbf{J}_s|\frac{\partial r}{\partial x_n} + r\frac{\partial |\mathbf{J}_s|}{\partial x_n}\right) d\xi$$
$$\frac{\partial (dV)}{\partial x_n} = \frac{\partial (r|\mathbf{J}|)}{\partial x_n} d\xi d\eta = \left(|\mathbf{J}|\frac{\partial r}{\partial x_n} + r\frac{\partial |\mathbf{J}|}{\partial x_n}\right) d\xi d\eta$$

where r is the radial position of the integration point.

After the sensitivities of the stiffness matrix and the nodal force vector are evaluated at the elemental level using Eq 7 and 8, they are assembled for the whole workpiece. A set of simultaneous linear algebraic equations is obtained as:

$$\bar{\mathbf{R}}\,\bar{\mathbf{V}}_{,p_l} = \bar{\mathbf{F}}_{,p_l} \qquad \text{(Eq 12)}$$

By solving the above equation, one can obtain the nodal velocity sensitivity $\partial \mathbf{V}/\partial p_l$.

3.2 *Boundary Conditions*

On the friction boundary, the traction is prescribed in the tangential direction, and the velocity is prescribed in the normal direction to the surface. The velocity boundary conditions of the ith node in contact with the dies are:

$$v_{i_n} = \mathbf{V}_{\text{die}}^T \cdot \mathbf{n} = (v_{\text{die}_x}, v_{\text{die}_y}) \begin{pmatrix} -\sin\beta \\ \cos\beta \end{pmatrix} \quad \text{(Eq 13)}$$

where v_{i_n} is the velocity component of the node i in the normal direction of the interface surface. $\mathbf{V}_{\text{die}}$ is the die velocity vector. $\mathbf{n}$ is the unit normal on the interface surface. β is measured from the x axis in the global coordinate system to the x' axis of the local coordinate system in counterclockwise direction. For a B-spline function defined by $y = y(p_l, x)$ $(l = 1, 2, \ldots, 2K)$, the slope of the B-spline curve is $dy/dx = y_x = \tan\beta$.

Differentiating Eq 13 with respect to the design variable p_l gives the following relationship:

$$\frac{\partial v_{i_n}}{\partial p_l} = \mathbf{V}_{\text{die}}^T \frac{\partial \mathbf{n}}{\partial p_l} = -v_{\text{die}_x} \frac{\partial \sin\beta}{\partial p_l} + v_{\text{die}_y} \frac{\partial \cos\beta}{\partial p_l} \quad \text{(Eq 14)}$$

where $\partial \mathbf{n}/\partial p_l$ is the sensitivity of the normal of the die surface to the design variable p_l. It can be obtained by differentiating the equation, which defines the normal of the B-spline curve. If node i is not in contact with the die that is being optimized, or if the dies are not optimized (for instance, during the final stage forging), then $\partial \mathbf{n}/\partial p_l = 0$.

4. Optimization Procedures

With the definition of a suitable objective and constraint functions and a method for obtaining sensitivity information, an optimization tool such as design optimization tool (DOT) (Ref 13) can be used to automate the shape design procedure. The optimization steps are described as follows:

1. Determine an initial guess of the preform die shape.
2. Perform the finite element analysis of the preforming stage. Calculate the nodal velocity sensitivities with respect to the design variables in each incremental simulation step after the finite element solution has converged. Update the nodal coordinate sensitivities.
3. Start the simulation of the final forging stage once the simulation of the preform stage is finished.
4. When the final stage simulation is finished, calculate the objective function gradients using the resulting nodal coordinate sensitivities and the objective function.
5. Call optimization program and check for optimization convergence. If further improvement is possible, then update the preform die shapes using the new control point coordinates provided by the optimization program. Repeat steps 2 through 5. If the optimality conditions are satisfied with the current shapes, the design objective is met.

5. Other Techniques

In the optimization of preform die shapes, several additional problems, such as remeshing, need to be solved in order to automate or improve the optimization process.

5.1 *Remeshing*

In practical metal forming processes, large deformations eventually lead to indeterminant elements when the determinant of Jacobian matrix becomes negative. Therefore, a new mesh of the workpiece must be defined and the history-dependent variables must be transferred to the new mesh system. The history-dependent field variables are effective strains, node temperatures (only for nonisothermal analysis) and the sensitivities of the node coordinates with respect to the design variables. These values must be defined on the new mesh by interpolation.

Sensitivities of the node coordinates with respect to the design variables are given at the node points. Thus, it is assumed that the distributions of node coordinate sensitivities within the workpiece domain can be expressed by using the element shape functions. Interpolation is done to evaluate the sensitivities at the new node locations.

5.2 *Adjustment of Volume Loss*

A small volume loss of the workpiece due to the geometry update within a finite time-increment is inevitable. In addition, the amount of volume loss will vary due to remeshing. Limiting the volume loss within a small percentage of the total deforming volume is a major consideration in the prediction of proper die fill and defect formation, which are important in process design. In a conventional finite element simulation, the amount of volume loss is controlled by limiting the maximum allowable time-increment and controlling remeshing.

The initial billet volume is determined to be equal to the final forging volume. However, with volume loss, the achieved final forging volume is always smaller than the initial billet volume. The objective function depends on the area of the zone where the two final forging shapes do not coincide. Therefore, the objective function is affected adversely by the volume loss. More importantly, the magnitude of volume loss may vary from one optimization iteration to another. This results in convergence problems when using the optimization algorithm.

To support design optimization, a volume loss adjustment procedure is incorporated in the simulation process. After each time-increment, the y-coordinates of the nodes in contact with the die surfaces are adjusted to ensure that the workpiece volume remains equal to the initial volume. At the same time, the die position is also adjusted by the same distance. After the adjustment, volume constancy is realized in every time-increment step. The final forging volume is exactly equal to the initial volume during the optimization iterations, and the convergence of the optimization procedure is improved significantly.

5.3 *Treatment of a Fold-Over Defect*

During the optimization design, the preform die shapes are updated after each iteration of optimization. The optimization tool gives the new coordinates of the control points according to the sensitivity and objective function information. Sometimes, the intermediate preform die shapes cause a fold-over defect in the final forging. This case usually occurs during intermediate optimization iterations while searching for the optimal preform die shapes. Therefore, measures need to be taken in order to correct the search direction to eliminate the defect while continuing the optimization process.

Once a fold-over is generated in the final forging for a particular intermediate preform die shape, the finite element analysis of the final forging process is stopped. A remeshing procedure is performed to generate a new mesh on the current workpiece. The boundary of the workpiece should be modified or smoothed in order to delete the fold-over defect before remeshing. This allows a new mesh to be generated on the workpiece without any fold-over defects. The finite element analysis is restarted again using the new mesh system. When the simulation of the final forging process is finished, values for the sensitivity and the objective function are calculated. Due to the presence of a defect, the objective function should be increased by a positive number, say, the maximum value of the objective functions among the previous optimization iterations. This number is used to penalize for the fold-over defect. The optimization tool uses this increased objective function to correct the searching direction by means of its self-correcting function. In this way, the finite element analysis is continued until the optimal preform die shapes are found.

6. Design Examples

In this work, the sensitivity analysis based preform die shape design method is used to design the preform die shapes of more complex forging processes including both plane strain and axisymmetric deformation modes. The goal is to design a preform die shape such that, after the final forging stage, a flashless forging with complete die fill is obtained. In each case, the forging process is considered to be isothermal. A non-strain-hardening material having the constitutive relation $\bar{\sigma} = Y_0\bar{\varepsilon}^{0.145}$ with $Y_0 = 33.99$ MPa was used in all design examples. A constant shear friction factor, $m = 0.2$, was assumed on the interface between the workpiece and the dies. In each case, the simulation contains only a top die, taking advantage of symmetric conditions, with a velocity of –1.0 mm/s.

6.1 *Plane Strain Deformation*

The final die shape is shown in Fig. 1. Only the top half of the model is considered for finite element analysis due to symmetry of the forging about the horizontal center line. Because the shape of the left cavity is different from that of the right cavity, the correct location of initial billet also needs to be determined along with the preform die shape. The initial billet is a bar with a square cross section. Given the initial guess of the preform die shape, the optimization is performed and the optimal preform die shape is determined via several optimization iterations.

Figure 1 shows the resulting preform shapes and the corresponding final forging shapes at various optimization iterations. In the first iteration, the left cavity of the final forging die is completely filled, but has large amount of flash. The right cavity is not completely filled. This indicates that the material distribution of the two cavities is not reasonable. In the second iteration, the right cavity is completely filled, with the existence of some flash. The left cavity is not completely filled. The third iteration generates a larger right flash than the second iteration. But after the third iteration, the right side flash is decreased gradually. After six iterations, the optimized preform die shape is obtained, which results in a final forging with complete die fill and no flash, as desired.

Figure 2 shows the objective function history over the optimization process. The objective function value is reduced to 2.92 mm^4, compared to a starting value of 98.67 mm^4, after six optimization iterations. For the third iteration, the objective function is the largest. This corresponds to the larger flash on the right side and the large underfill on the left side of the forging. The preform die shape at the sixth iteration can be selected as the optimal preform die shape, as the desired final shape is achieved using this preform die.

Figure 3 shows how the preform die shapes evolved with each optimization step. The dotted line shows the location center of the initial billet relative to the preform dies. It can be seen that the sensitivity analysis based preform die shape design also gives the optimal location of the initial billet in the preform die cavity. This aids in achieving a reasonable material distribution, which is very important in multicavity forging processes for obtaining an even flash distribution on the two sides and reducing die wear.

6.2 *Axisymmetric Deformation*

In this case, a preform die shape for achieving a flashless cross-sectional H-shaped axisymmetric forging is designed. For the H-shaped forging with ratio of cavity height to cavity width, $H/W = 2.0$, two stages should be used in order to get the final forging. In practical forging processes, the final forging usually has excessive flash due to the inappropriate design of

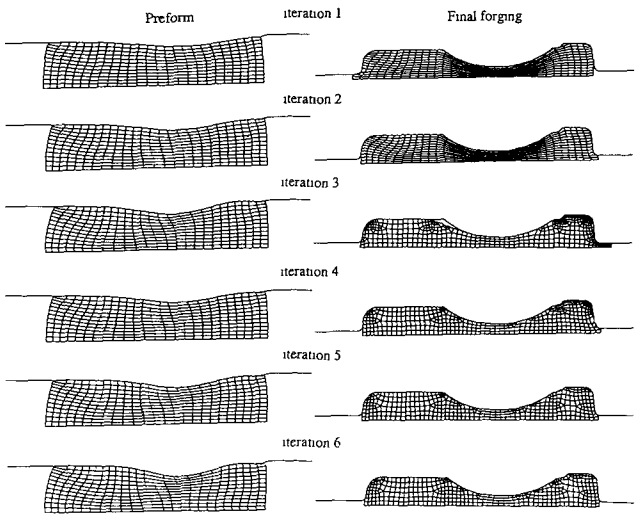

Fig. 1 Preform and final forging shapes for a plane strain forging

the preform die shapes. It is significantly important for reducing material waste as flash and excessive die wear to realize a flashless forging process. The elimination of the trimming stage may also be realized for a flashless forging.

The initial billet is a cylinder that has a diameter of 100 mm and a height of 100 mm. The mesh deformation patterns at the end of the preforming and final forging stages at each optimization iteration are shown in Fig. 4. For an initial guess of the preform die shape (iteration 1), the final forging has some flash and incomplete die fill. In the next three iterations, the die cavity fill is gradually improved. Correspondingly, the flash size is reducing iteration by iteration. This indicates that the optimization searching direction is correct. Therefore, in the fifth iteration, the optimization step size is increased, and the cavity of the preform die has a large slope. This preform die would increase the die fill and reduce the flash, but the workpiece in the finishing stage generates a fold-over defect. That means the preform die shape has been over-adjusted. After the fifth iteration, the preform die shape is adjusted back by the optimization tool. For the seventh iteration, the final forging die cavity is almost completely filled, and the forging is nearly flashless. After nine iterations, a flashless and completely filled final forging is achieved using the designed preform die shapes. Therefore, the preform die shape contained in ninth iteration is selected as the optimal one.

Figure 5 shows the objective function history over the optimization process. During the nine iterations, the objective function is reduced from 73.41 mm^4 to 1.24 mm^4. In this case, remeshing was needed for every iteration. The preform die shape iteration history for the axisymmetric problem is shown in Fig. 6.

From these two analysis cases, it can be concluded that the sensitivity analysis based preform die shape method provides a very effective tool for preform design engineering in metal forming. The preform dies designed by this method are easily manufactured and implemented because they do not contain any lateral concave die cavities. This is an important feature for utilizing this method in practical production applications. In this work, the desired forging shapes are always required to be flashless, which is a very strict objective. For complex forging problems, giving the desired forging a small or proper amount of flash will help to make the optimization process converge quicker. In fact, this is necessary for most practical forgings in industry. In a high volume production, the initial billet is usually prepared by bending, shearing, or sawing. The billet length or volume has a small tolerance, making the billet volume inconsistent from part to part. To ensure complete die fill, a small amount of flash added to the desired final forging shape will be helpful.

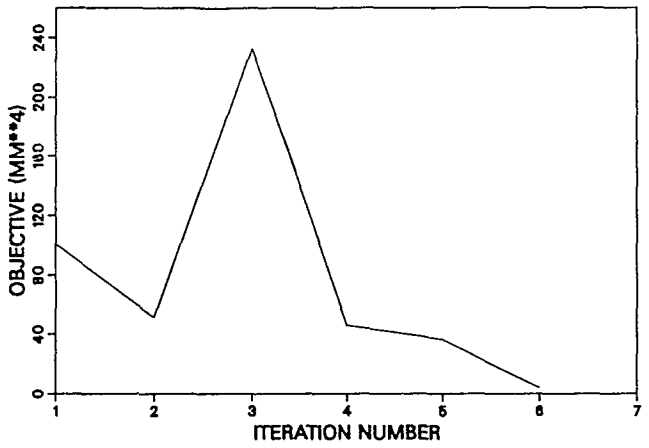

Fig. 2 Objective function versus optimization iterations for a plane strain forging

7. Conclusions

This paper used an optimization and sensitivity analysis based method to design the preform die shapes in forging processes. The method includes the determination of the objective function, sensitivity analysis, and the velocity boundary conditions. The optimization procedures, remeshing, volume loss adjustment, and treatment of fold-over defects were also described. Sensitivity of the objective function is calculated by the accumulated sensitivity of the nodal coordinates to the design variables throughout an entire simulation including the preforming and final forging processes.

The methodology was applied to the design of preform die shapes in both plane strain and axisymmetric forging problems containing a deep cavity. For plane strain deformation, the optimal preform die shape was designed, and the optimal billet location was also determined. Using the optimal preform die shape generated, the final forging was forged achieving complete die fill without any flash on either the left or the right side of the final part. For H-shaped ($H/B = 2$) axisymmetric forging problems, a flashless and completely filled final forging was produced using the optimized preform dies. Due to achieving a flashless forging, the forging load and die wear were significantly reduced, along with the possible elimination of the trimming stage and a reduction in machining cost. These result

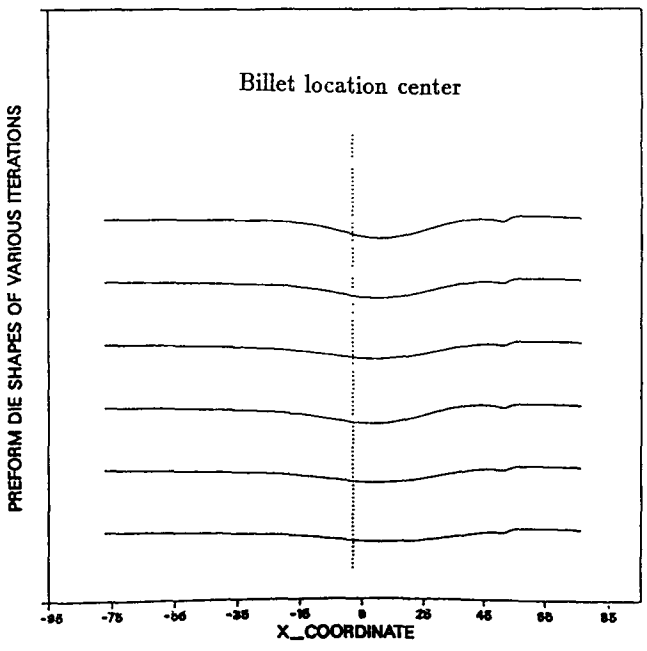

Fig. 3 Iteration history of the preform die shapes for a plane strain forging

methods indicate it to be a very effective one in realizing net-shape forging.

This work used only the difference between the desired and achieved final forging shapes as the design objective, that is, shape optimization. In fact, preform design is related to many process parameters, such as energy requirement, uniform deformation, and die wear. However, the authors believe that shape design is the most important parameter. Once the shape design method was found successful in preform design, the other parameters can be incorporated into the objective function to realize a multiobjective optimization of metal forming processes.

This paper concentrates on the preform die shape of forging processes. The authors believe that the method and ideas can also be applied to the preform design in sheet metal forming and three-dimensional problems.

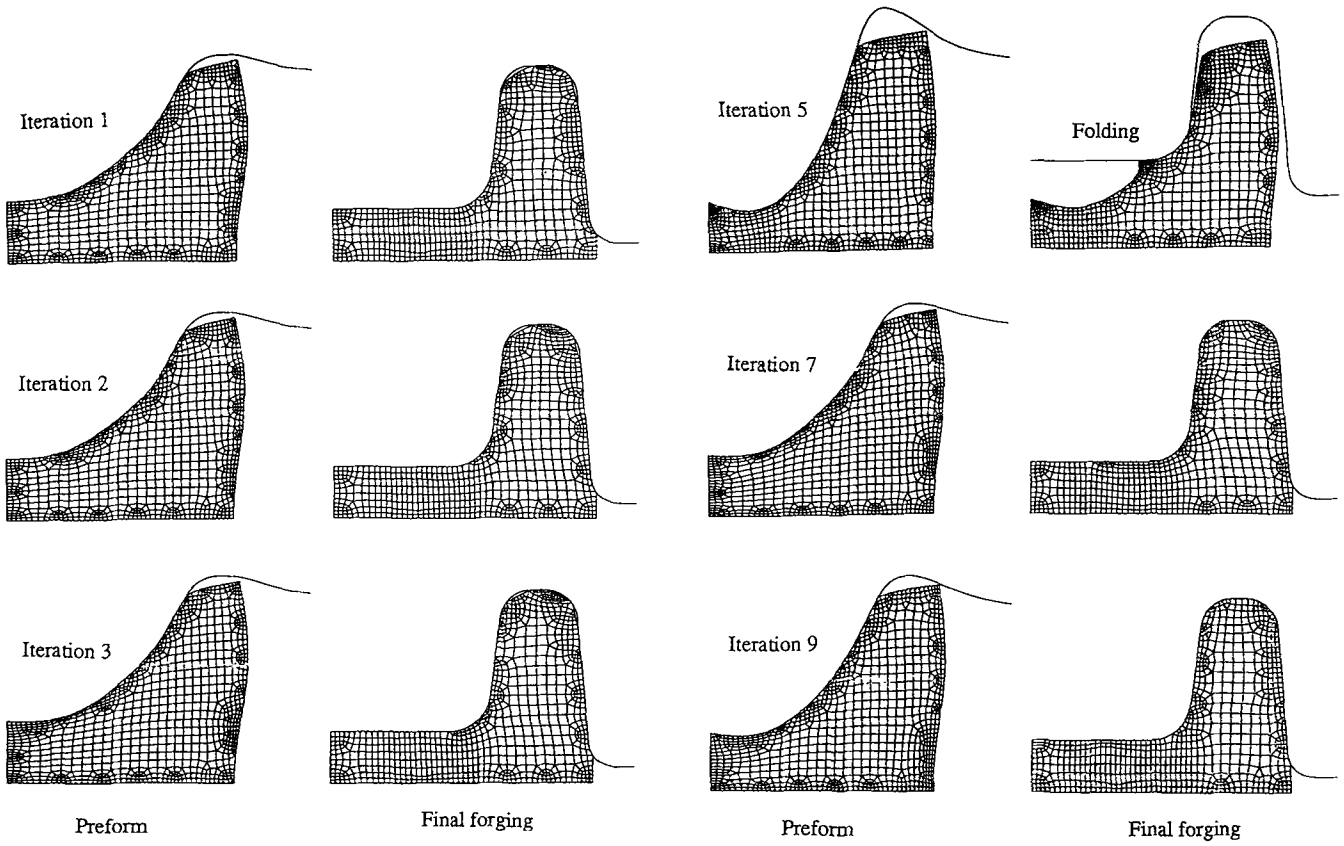

Fig. 4 Preform and final forging shapes for an axisymmetric forging of cross-sectional H-shape

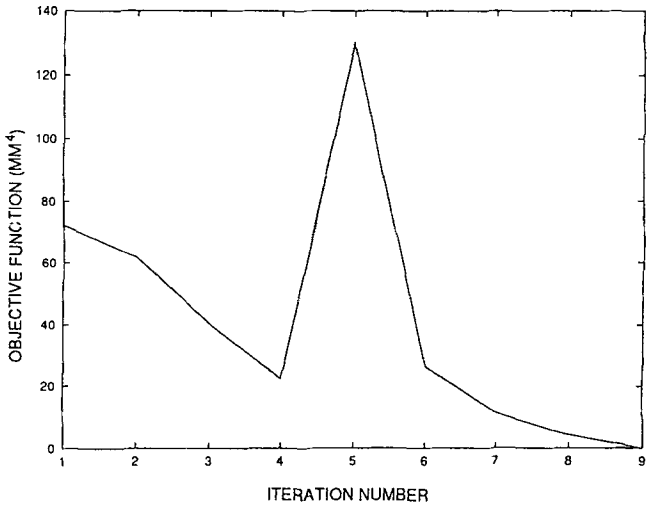

Fig. 5 Objective function versus optimization iterations for an axisymmetric forging of cross-sectional H-shape

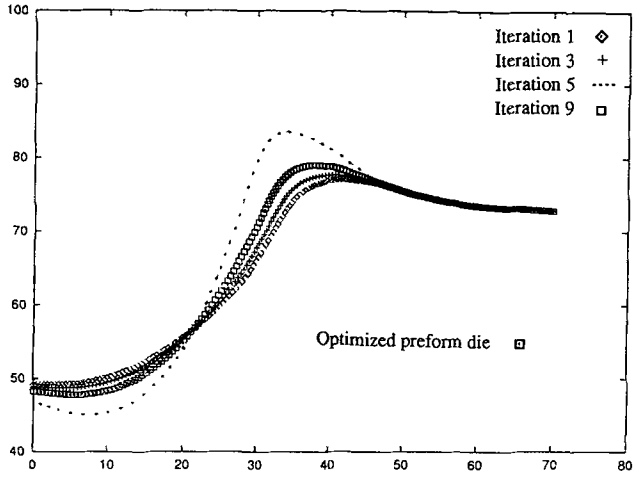

Fig. 6 Iteration history of the preform die shapes for an axisymmetric forging of cross-sectional H-shape

Acknowledgment

This research was supported by the National Science Foundation Grant DMI-9424649.

References

1. S. Kobayashi, S.I. Oh, and T. Altan, *Metal Forming and the Finite Element Method,* Oxford University Press, 1989
2. N. Kim and S. Kobayashi, Preform Design in H-Shaped Cross Section Axisymmetric Forging by Finite Element Method, *Int. J. Mach. Tools Manuf.,* Vol 31, 1991, p 243-268
3. B.S. Kang, N. Kim, and S. Kobayashi, Computer-Aided Preform Design in Forging of an Airfoil Section Blade, *Int. J. Mach. Tools Manuf.,* Vol 30, 1990, p 43-52
4. B.S. Kang and S. Kobayashi, Preform Design in Rolling Processes by the Three Dimensional Finite Element Method, *Int. J. Mach. Tools Manuf.,* Vol 31, 1991, p 139-151
5. G. Zhao, E. Wright, and R.V. Grandhi, Preform Design in Forging Processes Using Nonlinear Finite Element Method, *Trans. NAMRI/SME,* Vol 22, 1994, p 17-24
6. G. Zhao, E. Wright, and R.V. Grandhi, Forging Preform Design with Shape Complexity Control in Simulating Backward Deformation, *Int. J. Mach. Tools Manuf.,* Vol 35, 1995, p 1225-1239
7. G. Zhao, E. Wright, and R.V. Grandhi, Computer Aided Preform Design in Forging Using the Inverse Die Contact Tracking Method, *Int. J. Mach. Tools Manuf.,* Vol 36, 1996, p 755-769
8. S. Badrinarayanan and N. Zabaras, A Sensitivity Analysis for the Design of Metal Forming Processes, *Comput. Meth. Appl. Mech. Eng.,* Vol 129, 1996, p 319-348
9. L. Fourment, T. Balan, and J.L. Chenot, Shape Optimal Design in Forging, *NUMIFORM'95,* S.F. Shen and P.R. Dawson, Ed., A.A. Balkema/Rotterdam/Brookfield, 1995, p 557-562
10. G. Zhao, E. Wright, and R.V. Grandhi, Preform Die Shape Design in Metal Forming Using an Optimization Method, *Int. J. Numer. Methods Eng.,* (in press), 1997
11. G. Zhao, E. Wright, and R.V. Grandhi, Sensitivity Analysis Based Preform Die Shape Design for Net-Shape Forging, *Int. J. Mach. Tools Manuf.,* (in press), 1997
12. R. Fletcher, *Practical Methods of Optimization,* John Wiley and Sons, Inc., 1987
13. Vanderplaats Research & Development, Inc., *DOT Users Manual,* Version 4.20, Colorado Springs, CO, 1995